Optica Applicata, Vol. XXXVI, No. 2–3, 2006

Photoemission of 4*f* and 5*f* systems

ELŻBIETA GUZIEWICZ

Institute of Physics, Polish Academy of Sciences, al. Lotników 32/46, 02-668 Warsaw, Poland;
e-mail: Elzbieta.Guziewicz@ifpan.edu.pl

Photoemission studies provide an extensive insight into the electronic structure and are crucial for comprehension of the wide range of ground state properties found in lanthanide and actinide materials. This paper reviews different techniques used in photoemission experiments with respect to investigation of such specific aspects of the electronic structure of 4*f* and 5*f* systems as mixed valence, localization of 4*f* electron shell, and dual character of the 5*f* electrons. Photoemission results on lanthanide and actinide systems are also presented.

Keywords: photoemission spectroscopy, actinides, lanthanides, correlated electron systems.

1. Introduction

Photoemission spectroscopy (PES) is a direct and powerful probe of the occupied electronic structure, chemical properties of surfaces, and bonding in solids. The angle -resolved version of the technique (ARPES) provides unique information about $E(\overline{k})$ dependence which cannot be obtained by any other method. With PES experiment we are able to obtain information about the evolution of core levels and valence band as a fingerprint of chemical reactions on a surface; we can investigate the metal/semiconductor interface formation, or study the mixed-valence regime which occurs in some samarium, ytterbium, and europium compounds. PES is a very effective tool for studying materials containing the 4*f* and 5*f* electrons, especially when experiments are conducted on synchrotron radiation facilities. PES spectra allow distinguishing between highly localized (*e.g.*, the Gd 4*f*) and itinerant the 4*f* or 5*f* band (*e.g.*, the U 5*f*), and provide evidence for hybridization of the 5*f* electrons with a conduction band. In heavy fermions 5*f* materials the PES experiment is a valuable tool for evaluation of the various theoretical models that forms the foundation for a comprehensive understanding of complex solids.

This paper reviews different photoemission techniques used for investigation the 4*f* and 5*f*-based materials. In the next paragraph, the idea of photoemission spectroscopy will be described together with various modifications of this technique as XPS, UPS, SRPES, and ARPES. Section 3 deals with differences and similarities between the 4*f* electron shell in the lanthanides (called also rare earth, RE) and

the analogous 5*f* shell in the actinides. In Sections 4 and 5 the results of photoemission experiments on the 4*f* and the 5*f* systems are shown. We concentrate on photoemission investigations of such phenomena as a mixed-valence in 4*f*-based compounds, investigation of metal/semiconductor interface formation and studies of dual nature of the 5*f* systems. Summary of PES investigations of lanthanide- and actinide-based compounds is given in the last paragraph.

2. Photoemission spectroscopy

In a photoemission experiment we illuminate a sample with monochromatic radiation of the photon energy ranging between 20 and 1500 eV. The electrons excited by the photoelectric effect and situated near to the surface are liberated and detected in a kinetic energy analyzer. Figure 1 shows how the energy levels in the sample and the kinetic energy distribution, called the energy distribution curve (EDC), are related to each other. According to the three-step model of photoemission proposed by BERGLUND and SPICER [1], EDC is closely related to the density of states (DOS) of the material.

Three-step model divides photoemission process into three distinct and independent processes. In the first step the photon is absorbed and the electron is excited. The distribution of optically excited photoelectrons can be described by:

$$P(\hbar\omega, \overline{E}) \propto \sum_{i,f} \int d^3k \left|\langle f|\mathbf{p}|i\rangle\right|^2 \cdot \delta\left[E_f(\mathbf{k}) - E_i(\mathbf{k}) - \hbar\omega\right] \times \left[E_f(\mathbf{k}) - \overline{E}\right] \tag{1}$$

When *f* and *i* denote final and initial states, respectively, $\hbar\omega$ is photon energy and $\overline{E}$ is energy measured in a kinetic energy analyzer. Under assumption that the transition

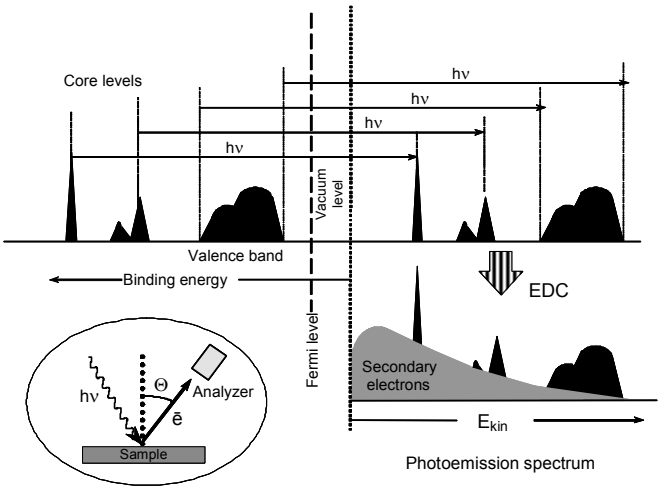

Fig. 1. The idea of the PES experiment.

matrix element $\langle f|\mathbf{p}|i\rangle$ is constant, the Eq. (1) is closely related to the joint density of states:

$$J(\hbar\omega) = \frac{1}{(8\pi)^3}\sum_{i,f}\int d^3k\cdot\delta\Big[E_f(\mathbf{k}) - E_i(\mathbf{k}) - \hbar\omega\Big] \tag{2}$$

In the second step of photoemission, excited photoelectrons travel to the surface. A part of photoelectrons lose their kinetic energy in elastic and inelastic collisions, and contribute to the secondary electron background observed in EDC spectra. The subtraction of the secondary electron background is the first step in examining of PES data. In this way only the signal from electrons which leave the sample without collisions during its travel to the surface is taken into account in PES spectra analyzes.

In the third step of photoemission, electrons escape through the surface into the vacuum where they are detected.

The three-step model is very useful in interpretation of PES results, in spite of the fact that the division of the photoemission process into three independent steps is quite artificial. However, the results obtained using the conceptually more complicated many-body one-step theory [2], are usually not very different. In the case of simple metals or semiconductors, it is generally assumed that a valence band photoemission spectrum reflects a final state screened by the charge equal to that being photo-emitted. For electron shell with strong correlation effects like 3*d* shell of transition metals (TM), 4*f* shell of lanthanides (La), and 5*f* shell of actinides (An) the final state effects are very strong and must be treated explicitly as the emission of one electron leads to excitation of the remaining system and to various final states with different energy. As a result, in the photoemission spectra of systems containing open *d* or *f* shells we observe characteristic multiplet structure. Generally speaking, additional lines (called also satellites) in PES spectrum are caused by different screening channels of the hole remaining in the systems after electron emission. Although it is not always easy to have a comprehensive understanding of all transitions involved, these processes should be taken into account when PES spectra of TM, La or An are analyzed.

In one-electron approximation described above, photoelectron spectroscopy (PES) is a "direct" experimental measurement of the energy levels or density-of-states (DOS) in a material. In interpretation of PES data within one-electron approach we should consider the photoionization cross-section dependences, which approximately account for neglected the transition matrix element.

PES is a surface sensitive spectroscopy as an escape depth of a photoelectron is only a few tens of monolayers. It is therefore essential to maintain ultra high vacuum (UHV) conditions to preserve the cleanliness of the crystal surface if the PES experiment is to be successful. Therefore the vacuum in the photoemission chamber is expected to be at the level 10^{-10}–10^{-11} torr and the sample under investigation has to be cleaned to remove the adsorbed contaminants in the PES chamber before the experiment. The common method of cleaning of polycrystalline samples is

scraping by a file or sputtering of the crystal surface by argon ions. For monocrystals the cleaving in the PES chamber seems to be the best method in which atomically clean surface is obtained.

2.1. XPS, UPS, and synchrotron radiation studies

The light source in PES experiment is an X-ray lamp, a gas-discharge helium (or hydrogen) lamp, or a synchrotron ring. Each radiation source provides different photon energy range and consequently introduces a specific potential in the electronic structure investigations.

In the X-ray photoemission spectroscopy (XPS) the X-ray lamp is used, which gives Al $K\alpha$ line with $h\nu = 1487$ eV. Such a high energy of radiation creates opportunity for exploring deep core levels, but it also results in a very poor energy resolution in the valence band region.

The ultraviolet photoemission (UPS) experiment is used to study the valence band region and shallow core levels with good energy resolution. The photon source in UPS is a helium gas-discharge lamp, which emits three resonant lines of He ($h\nu = 21.2$, 40.8, and 48.0 eV) situated in the ultraviolet (UV) range. Three photon energies enable us to study some photoionization cross-section dependences commonly used in PES experiments in order to determine contributions of specific electron shells to the EDC spectra.

New perspectives in PES studies were created when synchrotron light was used in the experiment. The synchrotron provides highly collimated light which covers a very broad spectral range from the visible to the X-rays, from which the specific photon energy can be extracted with monochromators. It this way we can achieve monochromatic and tunable photon source. Photon energy range accessible at photoemission stations in synchrotron radiation facilities usually varies between 20 and 200 eV, although there are experimental synchrotron photoemission stations where photon energy range is much higher (*e.g.*, BW2 station at HASYLAB where photon energy range is 2.4–25 kV). Tunable photon source provides exceptional possibilities in the PES investigations. The valence band and core level spectra can be measured at the same experimental set up using required photon energy. Photoionization cross-section dependencies can be exploited in more extensive range than it is in the UPS case. Resonant photoemission (RESPES), a very special tool of exploring the 3*d*, 4*f*, and 5*f* systems, can be applied only with the use of synchrotron radiation light. Tunable photon source allows us also to take complete advantage of angle-resolved photoemission (ARPES) which is described in the Sec. 4.

2.2. Angle-integrated and angle-resolved photoemission

In the inset of Fig. 1, the angle between a normal to the surface and the analyzer is marked as Θ. The kinetic energy analyzer used in a PES experiment is characterized by the so-called "acceptance angle" $\Delta\Theta$. If the acceptance angle of the analyzer is as high as several degrees, electrons with the same kinetic energy origin from different

parts of the Brillouin zone and then the results are interpreted in relation to the density of states and we have angle-integrated PES mode. In angle-resolved photoemission (ARPES) the acceptance angle of the analyzer is about 1°, therefore we measure the signal of electrons with almost the same **k** vector. When we collect spectra of different both photon energy and θ angle we can probe directly $E(\overline{k})$ dependence in the solid. Although a determination of the band structure from the obtained EDCs is not a trivial problem, the angle-resolved experiment generally allows us to have "direct" insight into the electronic band structure of the material.

3. The 4*f* and 5*f* electron systems

The lanthanide series is formed by the successive addition of a 4*f* electron to the electronic configuration of lanthanum. As 4*f* states are the first *f* states in the periodic table, the 4*f* wave functions have no nodes to ortogonalize them to the lower states. Therefore the 4*f* wave functions are contracted relatively to the *s* or *p* states. Thus the 4*f* shell of La usually is an inner and chemically inert shell. Anyway, there are some exceptions from this general rule as the 4*f* electrons in europium, samarium and ytterbium have larger spatial distribution and may participate in chemical bonding.

The actinides are more complex. In analogy with the lanthanides, the actinides are defined as the fourteen elements following actinium in the periodic table. The chemical properties of the early (light) actinides (from thorium through plutonium) are quite different from those of the next (heavy) actinides (americium through lawrencium). The 5*f* shells of the light actinides have larger spatial extent, are itinerant, participate in bonding, and affect most of the high-energy properties such as cohesion, crystal structure, and elastic properties. In contrast to those, the 5*f* electrons of the heavy actinides are localized, and the heavy actinides are the true counterpart to the La metals.

In the next paragraphs we will show how photoemission experiment can be applied to investigation of specific features of 4*f* and 5*f* based compounds.

4. Photoemission results on RE systems

4.1. Si:Gd alloy

The semiconductors containing La ions are of particular interest last days, because an atomic-like, compact 4*f* shell affects a variety of magneto-optical properties of the semiconductor system.

The $Si_{1-x}Gd_x$ alloys are of great interest since the giant magneto-resistance was found in this alloy and related to an exchange interaction between conduction electrons and the Gd 4*f* moments [3]. Similar phenomenon was expected for the other semiconductors containing Gd ions [4].

Figure 2 presents results of a synchrotron radiation study of the Si:Gd alloy containing about 1% of gadolinium. Photoemission spectra in Fig. 2**a** show the binding

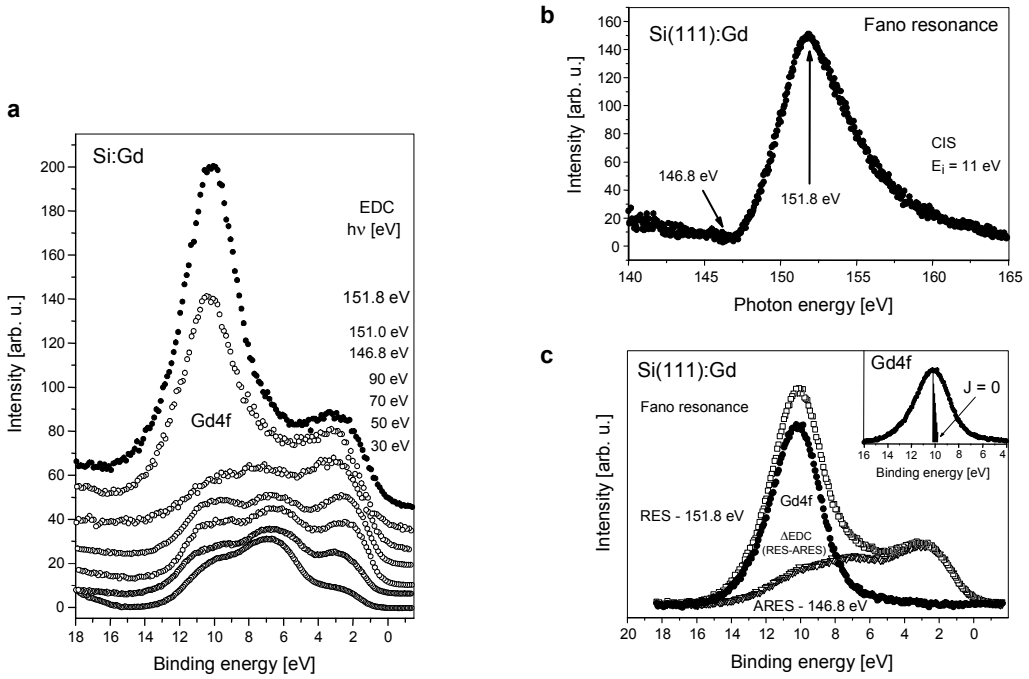

Fig. 2. Set of EDCs measured for Si:Gd alloy; binding energy covers the Si valence band and the Gd 4*f* shell – **a**. Constant initial state (CIS) spectrum shows the Fano resonance corresponding to the binding energy of the Gd 4*f* shell – **b**. The contribution of the Gd 4*f* electrons to the valence band spectra measured as a difference of the resonant and the anti-resonant EDCs [5] – **c**.

energy range between the Fermi level and 18 eV below, which covers the valence band region of silicon. The photon energy range is 30–152 eV which covers Gd 4*d*–Gd 4*f* absorption edge necessary to take advantage of the RESPES.

The RESPES method was designed to study the 3*d*, 4*f*, and 5*f* systems. The idea of this kind of photoemission experiment is explained on the example of the 4*f* system in Fig. 3. In a PES experiment we measure EDC spectra for photon energies near to the to the 4*d*-4*f* excitation threshold. At this threshold, the intensity of the photoemission current increases dramatically. It is because of the quantum interference between a direct and resonant photoemission processes. In the case of gadolinium these two photoemission channels can be describe as follows: the classical photoemission process from the Gd 4*f* shell

$$\mathrm{Gd}\ 4d^{10}4f^{7} + h\nu \rightarrow \mathrm{Gd}\ 4f^{6} + \bar{e} \tag{3}$$

is accompanied by the resonant photoemission from this shell

$$\mathrm{Gd}\ 4d^{10}4f^{7} + h\nu \rightarrow [\mathrm{Gd}\ 4d^{9}4f^{8}]^{*} \rightarrow \mathrm{Gd}\ 4d^{10}4f^{6} + \bar{e} \tag{4}$$

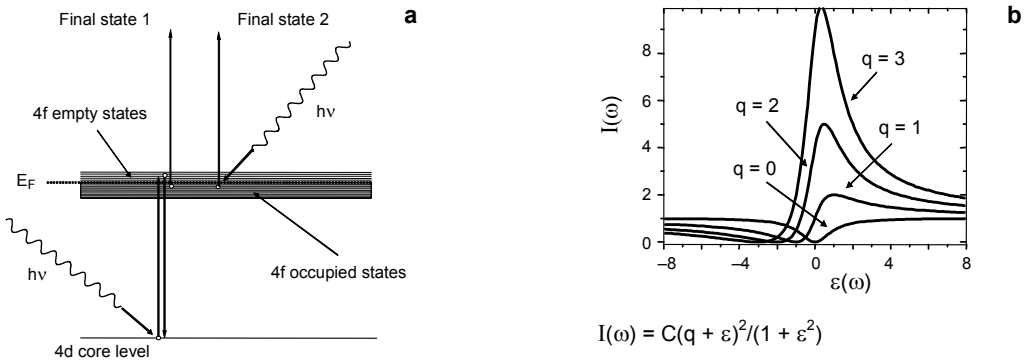

Fig. 3. The idea of the resonant photoemission (**a**), the shape of the Fano resonance (**b**).

As a result of the interference between two processes with the same initial and final states, we observe a strong and rapid variation of photoemission intensity from the Gd 4*f* shell. The phenomenon is based on the Fano effect [6]. The Fano effect was for the first time observed in photoemission in 1977 for NICKEL [7] and from that time is successfully used to investigate the position of the 3*d*, 4*f*, and 5*f* electrons in the electronic structure and to study hybridization of these electron shells with the ligand states.

The intensity of the photoemission near the absorption threshold has characteristic Fano-like shape with resonant maximum and anti-resonant minimum (Fig. 3**b**). We measure photoemission EDC spectra at a maximum and a minimum of the Fano resonance, which for gadolinium are 151.8 eV and 146.8 eV, respectively. Calculated difference spectra ΔEDC (EDC(151.8 eV) minus EDC(146.8 eV)) are related to the Gd 4*f* partial density of states. The result of subtraction is shown in Fig. 2**c**. The obtained ΔEDC curve shows the contribution of the Gd 4*f* electrons to the resonant photoemission spectra. In order to obtain the energy of $J = 0$ final state *vs.* the Fermi level, we deconvolute the ΔEDC spectra into the sum of components with $J = 0, 1, ..., 6$. The energy of the $J = 0$ initial state obtained in the procedure described above is equal 9.8 eV.

The results of RESPES studies of Si:Gd alloy show a highly localized Gd 4*f* electron shell and no evidence for hybridization with conduction electrons was found in the experiment.

4.2. Samarium deposited on GaN – a chemical reaction on the surface

Over the past decade the wide-gap semiconductor GaN has experienced significant attention due to its application in blue light emitting diodes and laser diodes. For the purpose of thin film optical emitters, the La doped GaN films offer a high potential with a full range of colors, a satisfactory quantum efficiency, and long term stability. Recently, richly structured luminescence spectra from Sm-implanted GaN epilayers

have been reported [8, 9]. High quantum efficiency indicates that samarium doped gallium nitride is a promising material for optoelectronic devices in the visible spectral range.

The 4*f* orbitals of La ions incorporated in semiconductors are usually deeply buried within the electronic structure and the $4f^n$ configurations are only slightly perturbed compared to free ion energy levels. As a consequence, the wavelength of La-related light emission is "atomic like" and almost insensitive to temperature, which is a very attractive attribute to light-emitting devices. A different situation, mixed-valence, occurs when the ionization energy of the 4*f* shell is very close to the chemical potential. This regime arises frequently in samarium compounds, where $Sm^{2+}(4f^6)$ and $Sm^{3+}(4f^5)$ configurations are almost degenerate and even small changes of chemical composition give rise to changes in the Sm valence. It also influences the light output as Sm^{3+} and Sm^{2+} ions produce quite different luminescence spectra [10].

In the experiment presented in Fig. 4 we sequentially deposited small amounts (from 0.6 to 20Å) of samarium on a clean GaN(000$\underline{1}$) surface under ultra-high vacuum and, via photoemission spectra, we followed changes in the Sm valence and the Ga 3*d* core level [11]. The purpose of the experiment was to investigate the interactions between samarium and gallium nitride in order to find out if both valence states can occur in the GaN matrix. The valence of samarium is easy to investigate by PES experiment, because Sm divalent and trivalent final states are characterized by distinct and well separated satellite spectral features. The multiplet structure corresponding to an initial $4f^6$ (Sm^{2+}) configuration (final state $4f^5$) has the most pronounced characteristic peak within –1 eV of the top of the valence band, while the multiplet associated with the $4f^5$ (Sm^{3+}) configuration (final state $4f^4$) appears between 5 and 10 eV below the Fermi level [12].

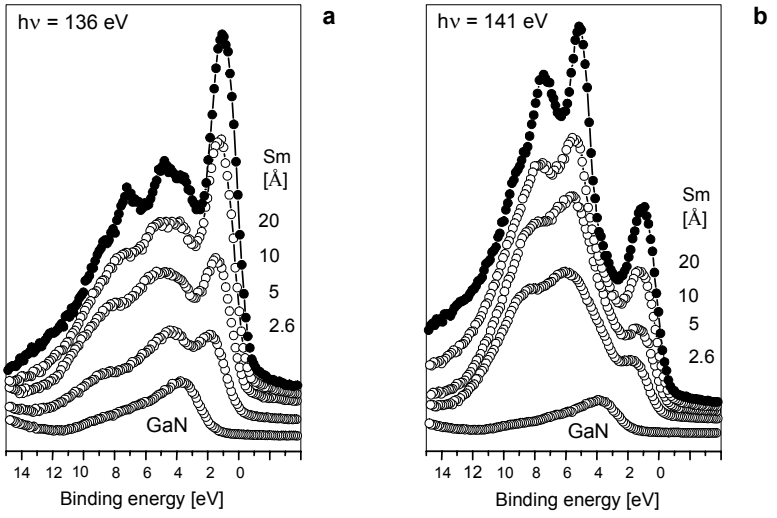

Fig. 4. Valence band EDCs for Sm/GaN(000$\underline{1}$) measured at: $h\nu$ = 136 eV (emphasize Sm^{2+} emission) – **a**, and $h\nu$ = 141 eV (emphasize Sm^{3+} emission) [11] – **b**.

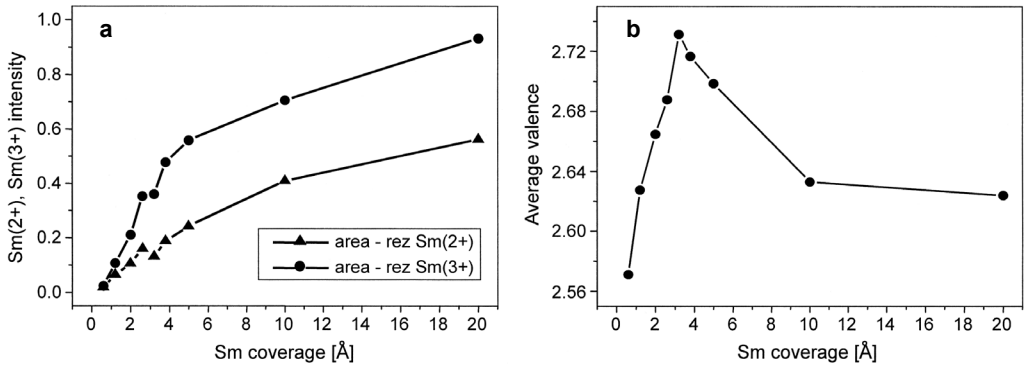

Fig. 5. Change in the Sm^{2+} and the Sm^{3+} photoemission intensity as a function of Samarium deposited on the surface of GaN(000$\underline{1}$) – **a**; an average Sm valence as a function of metal deposited on the surface [11] – **b**.

According to this, in RESPES experiment we observe two resonant maxima, one for $h\nu$ = 136 eV (corresponding Sm^{2+} configuration), and the second for $h\nu$ = 141 eV (corresponding Sm^{3+} configuration).

In Figure 4 we show two sets of EDCs measured for Sm/GaN system in the valence band region. Spectra in Fig. 4**a** were taken after each step of Sm deposition for photon energy of 136 eV and emphases the Sm^{2+} photoemission. Spectra in Fig. 4**b** were measured for $h\nu$ = 141 eV and emphases the Sm^{3+} photoemission. The analyzes of the shape of the EDCs from Fig. 4 lead to the conclusion that amount of both divalent and trivalent samarium valences increase with deposition up to 20 Å. It indicates the heterogeneous character of the interface. It is very useful to estimate the average valence of samarium in the Sm/GaN system as a function of samarium coverage in order to better understand the interactions in the system. The average valence we calculated using:

$$V_{\mathrm{avg}} = \frac{3I_3 + 2I_2}{I_3 + I_2} \tag{5}$$

where I_2 and I_3 denote the concentrations of the Sm^{2+} and Sm^{3+}. The concentrations can be deducted from resonant photoemission intensities. We calculate the ΔEDC spectra (analogically as it was shown for Gd 4*f* in the previous paragraph) for Sm^{2+} and Sm^{3+} resonance after each step of samarium deposition. We assumed that Sm^{2+} and Sm^{3+} contents were proportional to the ΔEDC(Sm^{2+}) and the ΔEDC(Sm^{3+}) integrals. The results of these calculations are shown in Fig. 5.

After each step of deposition we notice an increase of both divalent and trivalent samarium ions. However, the quantity of trivalent Sm atoms increases more rapidly than the divalent ones. Therefore the average valence of the system rises from 2.57 for coverage of 0.6 Å to 2.73 for coverage of 3.2 Å. Above 3.2 Å the valence drops and for coverage of 10 Å it is only 2.63. Above that coverage the average valence is

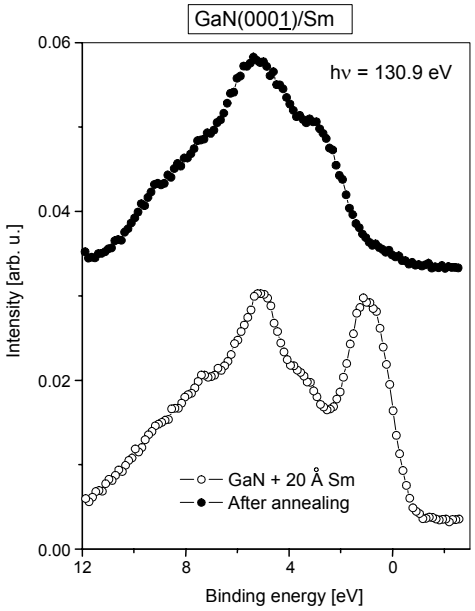

Fig. 6. Dramatic change of the valence band photoemission of the Sm/GaN system observed after annealing in 500°C. The EDC spectra were taken at anti-resonant photon energy (130.9 eV) [11].

almost stable. The gradual increase of signal from divalent samarium with deposition suggests that it originates not only from samarium atoms at the surface. If the origin of the Sm^{2+} photoemission intensity is only from samarium atoms at the surface, we would observe the saturation of this signal for complete coverage of the surface. It also should be noticed that the average valence in the GaN/Sm system is lower than for bulk samarium [12].

Some light can be shed on Sm–GaN interaction by the photoemission study taken after annealing of Sm/GaN interface to 500°C. To avoid the samarium oxides formation the annealing process was performed under ultra high vacuum conditions ($p \sim 10^{-10}$ torr). The EDC spectra taken after annealing (see Fig. 6) indicate that after annealing only trivalent Sm ions are present in the gallium nitride matrix. EDC spectra confirm that the divalent multiplet at the top of the valence band disappears after annealing as well as metallic shoulder at the Fermi edge. In the valence band region we see only features characteristic of trivalent Sm emission with the maximum at 5.4 eV. The average valence of the system increases considerably and reaches a value of 3. This indicates that annealing to 500°C leads to change of the valence of at least part of the divalent samarium which turns into trivalent and also promotes diffusion of divalent samarium from the surface into GaN matrix.

The photoemission results show that both divalent and trivalent Sm states coexist in the reactive GaN-Sm layer after each step of deposition, though the relation between them varies with coverage. The annealing of Sm/GaN system to 500°C induces a valence change from Sm^{2+} to Sm^{3+}.

In conclusion, Sm doped gallium nitride seems to be a good candidate for optoelectronic devices as it has mainly trivalent samarium which gives rich visible luminescence in the GaN matrix. One can eliminate some contribution of the divalent Sm by annealing the system to 500°C. However, the coexistence of both divalent and trivalent samarium ions in the GaN matrix before annealing provides evidence that in this case Sm $4f^6$ and Sm $4f^5$ configurations are almost degenerate. This creates some perspective for further studies towards application of GaN:Sm for 3D optical memory.

5. Photoemission results on actinide systems

The investigation of the 5*f* states in the actinide systems is an extremely interesting subject in the photoemission spectroscopy. Because of the large spatial extent of the 5*f* electron shell in the light actinides (thorium through plutonium), the wavefunctions of neighboring atoms overlap with each other and hybridize with the ligand states, but they are still at the border between localization and delocalization. The 5*f* electron shell with its "dual" character dominates to a large extent a great deal of unusual physical properties of these materials such as large anisotropic thermal-expansion coefficients, a dramatic drop in electrical resistivity at low temperature, and heavy fermion behavior [13–15]. The term "heavy fermions" is applied to materials whose electronic properties suggest the very heavy mass of the conduction electrons. The linear term of the specific heat, called a Sommerfeld coefficient γ, for some actinide compounds is as high as 1500 mJ/mole K^2. It suggests, within the Fermi-liquid theory that the electron mass by two orders of magnitude higher than that of the free electron. Magnetic susceptibility measurements generally show a Curie–Weiss behavior at elevated temperature, but below a characteristic temperature (usually referred to as the Kondo temperature T_K) the susceptibility levels off or even decreases. This is interpreted as a compensation of the magnetic moment by the ligand conduction electrons which align anti-parallel to the 5*f* electrons and form a singlet state [16]. At even lower temperature a dramatic drop in resistivity is observed. This is interpreted as a formation of a coherent periodic lattice of compensated *f* electrons, which is called the Kondo lattice or the Anderson lattice [17, 18]. The localized theoretical approaches like single impurity model (SIM) assume that even in periodic systems (*i.e.*, ordered compounds with the 5*f* electrons within each unit cell) the *f*-*f* overlap is very small, so the 5*f* electrons can be treated as completely localized impurities in the sea of ligand conduction electrons. As a consequence, the 5*f* electrons should not show any dispersion. Band approaches like periodic Anderson model (PAM) claim that the 5*f* electrons form Bloch states and very narrow bands at all temperature range [19, 20], so they show E versus k dependence. At the focus of the issue is the role of the 5*f* electrons in the formation of the heavy fermion state.

In general, the photoemission experiment is able to distinguish between localized and band states as in the latter case the $E(k)$ dispersion is expected. The problem is in the experimental resolution because a dispersion of the *f* state at low temperature (*i.e.*, in a coherent state) predicted by PAM model is to be of the order of T_K. This makes

the problem very difficult to solve in practice. In the abundant photoemission experiments, which were taken in late 80's and early 90's [21–24] the dispersion of the 5*f* bands was not observed. Most of these experiments were performed on polycrystalline samples and experimental resolution was in some cases lower by an order of magnitude than the features under study.

The considerable advances in the quality of the actinide samples and in the experimental resolution led to new experimental results, which seem to suggest that the localized treatment of the 5*f* electrons is less than perfect. In the next paragraph the PES results of two uranium compounds USb_2 and UAsSe will be shown together with related dispersions in the $E(k)$ dependence.

5.1. Band dispersions in USb_2

Below the temperature $T_N = 206$ K USb_2 is antiferromagnet. The relatively highly ordered magnetic moment (1.68 μ_B/U [25]) accounts for the localization of the U 5*f* shell.

The USb_2 photoemission spectra taken for photon energy of 34 eV are presented in Fig. 7 [26]. The sample used in the experiment was a single crystal, oriented by X-ray diffraction and cleaved under ultrahigh vacuum conditions to obtain smooth and flat surface for ARPES studies. The binding energy range in Fig. 7 covers only 0.7 eV below the Fermi level. This narrow binding energy range is related to the range of expected dispersions and is considerably narrower than the binding energy range usually measured for the 4*f* and 3*d* electron-based materials (compare energy range in Figs. 2, 4, 6 and 7). In the PES investigations of the 5*f* electrons, we are

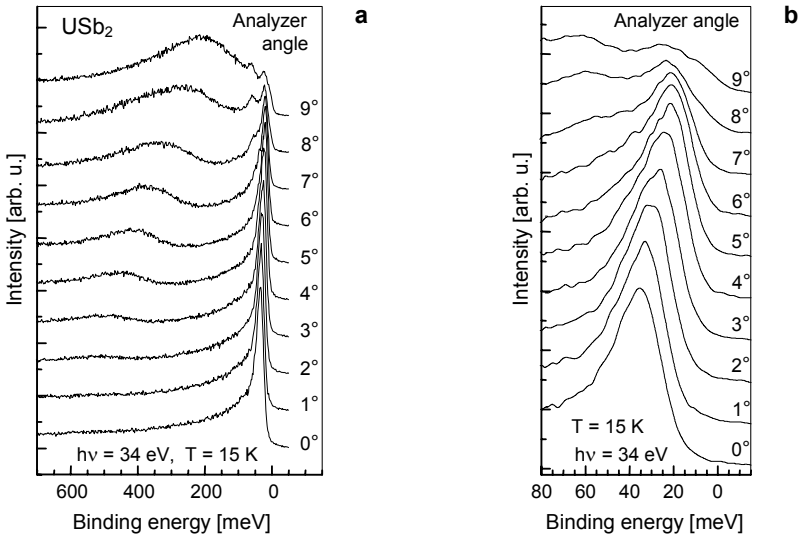

Fig. 7. High-resolution angle-resolved spectra of USb_2 were taken within 0.7 eV (**a**) and 0.08 eV (**b**) of the Fermi edge [26].

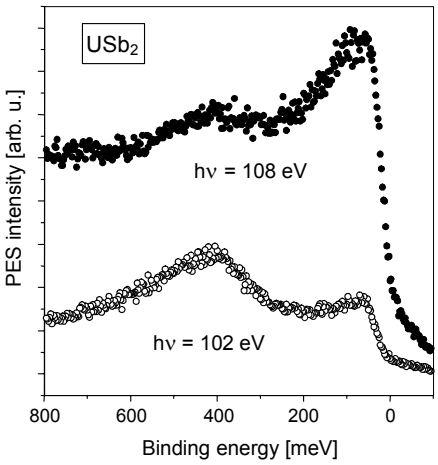

Fig. 8. RESPES spectra of USb_2 taken for U $5d \rightarrow$ U $5f$ absorption threshold show a resonant enhancement of photoemission features within 700 meV of the Fermi edge [26].

looking for the very subtle effects in the $E(k)$ dependence. Therefore the investigated binding energy range has to be narrow, and the excellent experimental resolution is crucial for the successful observation of the expected $5f$ dispersions.

Because of the very narrow binding energy range analyzed in the $5f$ material investigations, we do not need to bother about the satellite structures, which appear in a higher binding energy region as it was already mentioned in Sec. 2.

The overall energy resolution in USb_2 crystal investigations varied between 24 meV (for $h\nu = 34$ eV) and 49 meV (for $h\nu = 60$ eV). The momentum resolution at $h\nu = 30$ eV was 0.09 $Å^{-1}$, which was between 6% and 12% of the Brillouin zone depending on the investigated direction. An extremely good experimental resolution and small lifetime broadening allow observation of dispersion in the U $5f$ bands. The EDC spectra presented in Fig. 7**a** show two distinct photoemission features. One of them is a broader (FWHM about 150 meV) structure with dispersion of about 300 meV. The main feature of the EDCs is a sharp peak situated near to the Fermi level. This sharp peak also shows dispersion as can be seen in Fig. 7**b**, where narrower binding energy range is presented. The dispersion, as seen by numerical fitting was found to be 14 meV. The results of RESPES study presented in Fig. 8 [26] show a resonant enhancement in the binding energy region of both structures observed in Fig. 7**a**. The results of RESPES studies indicate that both structures observed within 700 meV of the Fermi edge are of the $5f$ origin.

The full width at half maximum (FWHM) of the $5f$ feature observed near to the Fermi level is about 24 meV and it is the sharpest photoemission feature found in uranium compounds up to date. The natural linewidth is conservatively estimated to be less than 10 meV when instrumental resolution is removed. In reality natural FWHM may very possibly be much smaller than 10 meV.

The ARPES studies of USb_2 crystal unambiguously show the dispersion of the hybridized U 5*f* bands. The PES results confirm that this 5*f* electron system needs to be described by periodic theoretical models.

It is worth to notice that the value of observed dispersion (14 meV) is indeed very small. To observe it we need to use the sophisticated photoemission set-up, which assures a very high energy resolution. To have the taste of the problem we can compare the binding energy scale in Figs. 2 and 4 with the binding energy scale in Fig. 7**b**. In the former case (spectra of the Si:Gd alloy and the GaN/Sm system) experimental resolution was about 0.3 eV, which was enough to investigate these systems. In the latter case (USb_2 single crystal) the total binding energy scale was much lower than 300 meV resolution used in the former case. This explains why in photoemission experiments, which were taken in late 80's and early 90's [21–24] the dispersion of the 5*f* bands was not observed.

5.2. Dual character of the 5*f* electrons in UAsSe

Uranium arsenoselenide is a very interesting subject of the electronic structure investigations because the optical and transport investigations lead to ambiguous conclusions in respect to the localization of the U 5*f* electrons. UAsSe is a hard ferromagnet with T_c temperature between 102 and 118 K (it depends on the As/Se molar ratio). Magnetic susceptibility measurements [27] and polarized diffraction studies [28] appear to point out the localization of the U 5*f* electrons in UAsSe. On the other hand, the enhanced Sommerfeld coefficient (reported between 20 and 40 mJ/mol K) and magneto-optical Kerr spectra [29] provide evidence for some degree of itinerancy of the 5*f* shell. UAsSe seems to combine aspects of the dual nature of the 5*f* electrons in one material.

UAsSe crystallizes in the tetragonal PbFCl-type crystal structure (Fig. 9**a**). This type of the crystallographic cell can be regarded as a stack of layers along

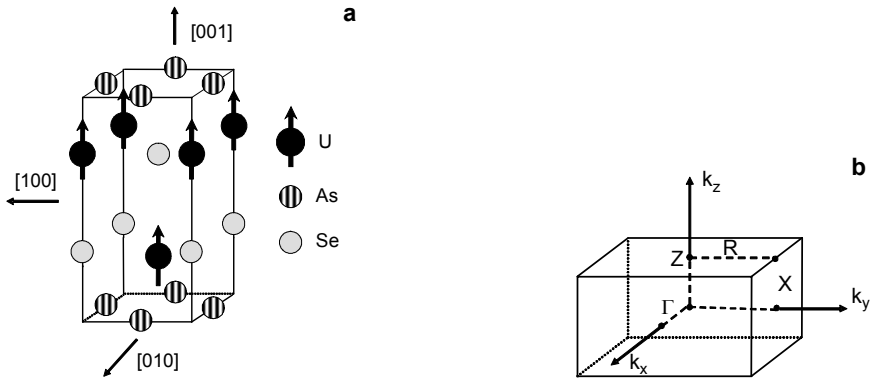

Fig. 9. Unit cell of UAsSe crystal structure with the magnetic moments on uranium sites indicated by arrows (**a**). Brillouin zone of UAsSe (**b**).

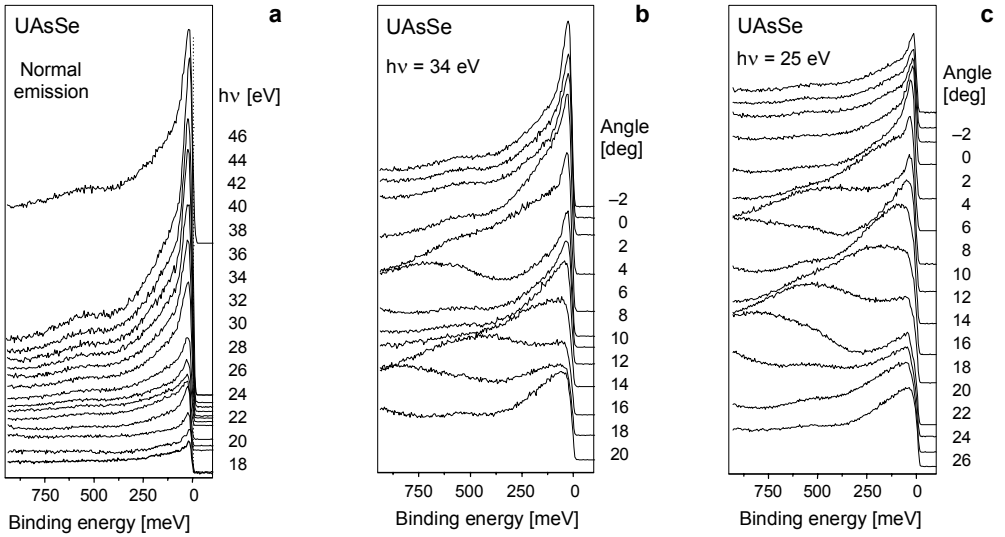

Fig. 10. High-resolution ARPES spectra of UAsSe taken along the different directions of the Brillouin zone [30]: Γ to Z (**a**), Z to R (**b**), Γ to X (**c**).

the c direction, which is also the easy magnetic axis. The Brillouin zone of UAsSe is shown in Fig. 9**b**.

High-resolution ARPES spectra of UAsSe along Γ to Z, Z to R, and Γ to X directions of the Brillouin zone are presented in Figs. 10**a**, 10**b**, and 10**c**, respectively. The picture of the electronic structure of UAsSe concluded from ARPES studies partially presented in Fig. 10 may be described as follows. Within 50 meV of the Fermi edge we observe a slightly dispersive peak with Lorenzian FWHM of 35 meV. This narrow band is mainly of 5f-character as was established based on resonant photoemission and cross-section dependencies. The dispersion, as seen from numerical fitting, is 40 meV along both the Γ to X and Z to R directions, and about 30 meV along the Γ to Z direction in the Brillouin zone. Apart from the narrow band, at least two broader bands of hybridized f-d character are observed. These two bands show conventional, high dispersion of 1 eV along Γ to X and Z to R directions, but no dispersion along the Γ to Z direction is observed. ARPES results indicate that the 5f electrons in the uranium plates (Γ to X and Z to R directions) are rather delocalized, while being quite well localized in the perpendicular direction (*i.e.*, along the c axis).

ARPES measurements presented in Fig. 10 reveal intriguing properties of the f electrons in UAsSe. For the first time the well localized, narrow bands of f-character and highly dispersive hybridized d-f bands were found inside the same 5f-material. This observation beautifully reflects the dual nature of actinide f-electrons, which was postulated in the literature many years ago [31].

It should be noticed that the fingerprints of co-existence of localized and itinerant $5f$ states has been recently postulated for δ-plutonium [32] and plutonium-based superconductor $PuCoGa_5$ [33]. Angle-integrated photoemission spectra of δ-Pu and $PuCoGa_5$ can be reproduced so far only within so-called the mixed level model (MLM) [32, 33]. The basis of the MLM is a partitioning of the electron density into localized and delocalized parts and minimizing the total energy with respect to this partitioning. For both Pu-systems the minimum is achieved for the four $5f$ electrons localized and roughly one in a delocalized Bloch state. Unfortunately, high-resolution ARPES synchrotron radiation band structure investigations cannot be performed for Pu and Pu-based compounds. Because of extremely high radioactivity these materials are not allowed to be measured in synchrotron radiation facilities.

6. Summary

Photoemission spectroscopy provides a variety of information about the $4f$ and $5f$ systems. With the extensive use of synchrotron radiation this method can be employed for such diverse kind of studies as investigation of the chemical properties of surfaces, determining the $4f$ or $5f$ energy with respect to the Fermi level, their hybridization with the ligand states, and study of dispersion relations of the $5f$ electronic states. In the case of $5f$ systems photoemission spectroscopy provides information necessary to evaluate various theoretical models and thus contributes to their development as the evolution of theoretical models is driven mainly by experiment.

Acknowledgements – The author thanks very much Bronek Orlowski and Bogdan Kowalski from the Institute of Physics Polish Academy of Sciences for cooperation in semiconductor materials investigations. Thanks are due to the photoemission team from Los Alamos National Laboratory (John Joyce, Tomek Durakiewicz, Martin Butterfield, and Al Arko) and Clifford Olson from Ames Laboratory for cooperation in the actinide compounds studies.

References

[1] BERGLUND C.N., SPICER W.E., *Photoemission studies of copper and silver: theory*, Physical Review **136**(4A), 1964, pp. A1030–44.

[2] FADLEY C.S., [In] *Electron Spectroscopy: Theory, Techniques and Applications II*, [Ed.] C.R. Brundle, Academic, New York 1978.

[3] HELLMAN F., QUEEN D.R., POTOK R.M., ZINK B.L., *Spin-glass freezing and RKKY interactions near the metal-insulator transition in amorphous Gd-Si alloys*, Physical Review Letters **84**(23), 2000, pp. 5411–4.

[4] STORY T., GÓRSKA M., ŁUSAKOWSKI A., ARCISZEWSKA M., DOBROWOLSKI W., GRODZICKA E., GOŁACKI Z., GAŁĄZKA R.R., *New mechanism of f-f exchange interactions controlled by Fermi level position*, Physical Review Letters **77**(16), 1996, pp. 3447–50.

[5] ORLOWSKI B.A., GUZIEWICZ E., NOSSARZEWSKA-ORLOWSKA E., BUKOWSKI A., JOHNSON R.L., *Photoemission study of Gd on clean Si(111) surface*, Surface Science **507–510**, 2002, pp. 218–22.

[6] FANO U., *Effects of configuration interaction on intensities and phase shifts*, Physical Review **124**, 1961, pp. 1866–78.

[7] GUILLOT C., BALLU Y., PAIGNÉ J., LECANTE J., JAIN K.P., THIRY P., PINCHAUX R., PETROFF Y., FALICOV L.M., *Resonant photoemission in nickel metal*, Physical Review Letters **39**(25), 1977, pp. 1632–5.

[8] GRUBER J.B., ZANDI B., LOZYKOWSKI H.J., JADWISIENCZAK W.M., *Spectroscopic properties of Sm^{3+} ($4f^5$) in GaN*, Journal of Applied Physics **91**(5), 2002, pp. 2929–35.

[9] LOZYKOWSKI H.J., JADWISIENCZAK W.M., BROWN I., *Cathodoluminescence of GaN doped with Sm and Ho*, Solid State Communications **110**(5), 1999, pp. 253–8.

[10] RIBEIRO C.T.M., ALVAREZ F., ZANATTA A.R., *Red and green light emission from samarium-doped amorphous aluminum nitride films*, Advanced Materials **14**(16), 2002, pp. 1154–7.

[11] GUZIEWICZ E., KOWALSKI B.J., ORLOWSKI B.A., SZCZEPANSKA A., GOLACKI Z., KOWALIK I.A., GRZEGORY I., POROWSKI S., JOHNSON R.L., *Interaction between Sm and GaN-a photoemission study*, Surface Science **551**(1–2), 2004, pp. 132–42.

[12] STRISLAND F., RAMSTAD A., BERG C., RAAEN S., *Valence variations in the monolayer regime of Sm on the Nb(110) surface*, Surface Science **410**(2–3), 1998, pp. 344–50.

[13] OTT H.R., FISK Z., *Handbook on the Physics and Chemistry of the Actinides*, [Eds.] A.J. Freeman, G.H. Lander, Noth-Holland, Amsterdam 1987, pp. 85–225.

[14] HESS D.W., RISEBOROUGH P.S., SMITH J.L., *Encyclopedia of Applied Physics*, [Ed.] G.L. Trigg, Vol. 7, VCH Publishers, NY 1993, pp. 435–63.

[15] STEWART G.R., *Heavy-fermion systems*, Reviews of Modern Physics **56**(4), 1984, pp. 755–87.

[16] GREWE N., STEGLICH F., *Handbook on the Physics and Chemistry of the Rare Earth*, [Eds.] K.A. Gschneider Jr., L. Eyerling, Vol. 14, North-Holland, Amsterdam 1991, pp. 343–474.

[17] LAWRENCE J.M., MILLS D.L., *Recent progress in heavy fermion/valance fluctuation physics: introduction*, Comments on Condensed Matter Physics **15**(3), 1991, pp. 163–74.

[18] LEE P.A., RICE T.M., SERENE J.W., SHAM L.J., WILKINS J.W., *Theories of heavy-electron systems*, Comments on Condensed Matter Physics **12**(3), 1986, pp. 99–161.

[19] ZWICKNAGL G., *Quasi-particles in heavy fermion systems*, Advances in Physics **41**(3), 1992, pp. 203–302.

[20] SHENG Q.G., COOPER B.R., *Non-Kondo prediction of Wilson ratio for heavy fermion systems*, Philosophical Magazine Letters **72**(2), 1995, pp. 123–34.

[21] ALLEN J.W., OH S.J., GUNNARSSON O., SCHONHAMMER K., MAPLE M.B., TORIKACHVILI M.S., LINDAU I., *Electronic structure of cerium and light rate-earth intermetallics*, Advances in Physics **35**(3), 1986, pp. 275–316.

[22] PATTHEY F., SCHNEIDER W.D., BAER Y., DELLEY B., *High-temperature collapse of the Kondo resonance in $CeSi_2$ observed by photoemission*, Physical Review Letters **58**(26), 1987, pp. 2810–3.

[23] MALTERRE D., GRIONI M., WEIBEL P., DARDEL B., BAER Y., *Evidence of a Kondo scale from the temperature dependence of inverse photoemission spectroscopy of $CePd_3$*, Physical Review Letters **68**(17), 1992, pp. 2656–9.

[24] LIU L.Z., ALLEN J.W., GUNNARSSON O., CHRISTENSEN N.E., ANDERSEN O.K., *α-γ transition in Ce: a detailed analysis of electron spectroscopy*, Physical Review B: Condensed Matter **45**(16), 1992, pp. 8934–41.

[25] SANTINI P., LEMANSKI R., ERDŐS P., *Magnetism of actinide compounds*, Advances in Physics **48**(5), 1999, pp. 537–653.

[26] GUZIEWICZ E., DURAKIEWICZ T., BUTTERFIELD M.T., OLSON C.G., JOYCE J.J., ARKO A.J., SARRAO J.L., MOORE D.P., *MORALES L., Angle-resolved photoemission study of USb_2: the 5f band structure*, Physical Review B: Condensed Matter and Materials Physics **69**(4), 2004, pp. 45102-1–8.

[27] HENKIE Z., FABROWSKI R., WOJAKOWSKI A., ZALESKI A.J., *Suppression of the ferromagnetic state by disorder in the anisotropic Kondo lattice system UAsSe*, Journal of Magnetism and Magnetic Materials **140–144**, 1995, pp. 1433–4.

[28] WIŚNIEWSKI P., GUKASOV A., HENKIE Z., WOJAKOWSKI A., *Polarized neutron diffraction study of spin and orbital moments in UAsSe*, Journal of Physics: Condensed Matter **11**(33), 1999, pp. 6311–7.

[29] OPPENEER P.M., BROOKS M.S.S., ANTONOV V.N., KRAFT T., ESCHRING H., *Band-theoretical description of the magneto-optical spectra of UAsSe*, Physical Review B: Condensed Matter **53**(16), 1996, pp. R10437–40.

[30] GUZIEWICZ E., DURAKIEWICZ T., OPPENEER P.M., JOYCE J.J., THOMPSON J.D., OLSON C.G., BUTTERFIELD M.T., WOJAKOWSKI A., MOORE D.P., ARKO A.J., *Angle-resolved photoemission study of dispersive and narrow-band 5f states in UAsSe*, Physical Review B: Condensed Matter and Materials Physics **73**(15), 2006, pp. 155119-1–10.

[31] FREEMAN A.J., KOELLING D.D., [In] *The Actinides: Electronic Structure and Related Properties*, [Eds.] A.J. Freeman, J.B. Darby Jr., Academic Press, New York 1974.

[32] WILLS J.M., ERIKSSON O., DELIN A., ANDERSSON P.H., JOYCE J.J., DURAKIEWICZ T., BUTTERFIELD M.T., ARKO A.J., MOORE D.P., MORALES L.A., *A novel electronic configuration of the 5f states in delta-plutonium as revealed by the photoelectron spectra*, Journal of Electron Spectroscopy and Related Phenomena **135**(2–3), 2004, pp. 163–6.

[33] JOYCE J.J., WILLS J.M., DURAKIEWICZ T., BUTTERFIELD M.T., GUZIEWICZ E., SARRAO J.L., MORALES L.A., ARKO A.J., ERIKSSON O., *Photoemission and the electronic structure of* $PuCoGa_5$, Physical Review Letters **91**(17), 2003, pp. 176401/1–4.

Received December 15, 2005
in revised form July 31, 2006